The International Journal of Advanced Manufacturing Technology (2020) 110:481–498
https://doi.org/10.1007/s00170-020-05796-8

ORIGINAL ARTICLE

Modeling the electrical power and energy consumption of automated guided vehicles to improve the energy efficiency of production systems

Matthias Meißner[1] · **Lynn Massalski**[1]

Received: 23 April 2020 / Accepted: 17 July 2020 / Published online: 13 August 2020

Abstract

Due to the advancing energy system transformation and the increasingly complex and dynamic environment in which factories have to operate, the energy efficiency and flexible design of production systems are becoming more important. Since the use of automated guided vehicles is a promising approach to enhance the flexibility of intralogistics, their electrical power requirements are analyzed. Based on the measurement data obtained, different movement modules of an automated guided vehicle are identified and then modeled using physical laws. These movement modules are the translatory movement, rotary movement, and the lifting and lowering of the load-carrying platform. The measurement data show, for example, that the energy requirement for translational and rotational movement increases in relation to the payload weight. At the same time, however, it is also shown that an increase in speed of the automated guided vehicle leads to a lower energy requirement, although the power requirement grows. Consequently, one result is that an automated guided vehicle works most efficiently when the maximum payload is transported at the highest speed. With regard to the lifting and lowering of loads, the result is an increasing energy requirement depending on the payload weight. The comparison between the collected measurement data and the outcomes of the implemented simulation model shows only minor deviations. Thus, the implemented simulation model of automated guided vehicles can be used with regard to their electrical power consumption, for example, in production planning to comprehensively raise the energy efficiency of production systems.

Keywords Energy efficiency · Intralogistic · Automated guided vehicles · Factory modeling

1 Introduction

In addition to the expansion of renewable energy sources, increasing energy efficiency is a central aspect of the energy system transformation. The objective is to reduce the primary energy consumption of all sectors (industry, services and commerce, private households, transport) [1, 2]. For instance, energy efficiency in the European Union is to be increased by 27% by the year 2050 in order to reduce primary energy requirements [3]. The industrial sector in particular shows great potential for this [4, 5]. In order to exploit this potential, however, it is necessary to know the energy requirements of production processes in detail [6]. All types of production processes must be taken into account, such as material transforming processes, energy converting processes or logistic processes. Only then a comprehensive optimization of energy efficiency for a production system can be realized.

Besides the energy turnaround, which sets new challenges for industry, the surrounding of factories is becoming increasingly dynamic and complex [7]. For example, the lot size to be produced is becoming smaller and smaller. For this reason, production systems have to be arranged increasingly flexible. In order to achieve this objective and to meet these challenges, the current industrial development provides new possibilities [4, 6, 8]. A concrete opportunity for industrial development is the introduction and application of adaptive production systems [9, 10]. These systems, for example, enable detailed monitoring of all relevant production variables, such as electrical power

✉ Matthias Meißner
matthias.meissner@tu-dortmund.de

Lynn Massalski
lynn.massalski@tu-dortmund.de

[1] Institute of Energy Systems, Energy Efficiency and Energy Economics, TU Dortmund University, Emil-Figge-Straße 70, 44227 Dortmund, Germany

consumption, through their distinctive sensor technology. Electrical energy data in particular are typically not recorded in real time, but are only subsequently collected by the energy supplier via billing. Consequently, it is often not possible to take these data into account in a real-time control of production systems, which is why energy efficiency currently is still a subordinate optimization objective in production planning [6, 11]. In the context of adaptive production systems and the real-time control of these, it is of interest to include the electrical power consumption of all operating resources in the decision-making process.

Intralogistic is of particular interest for the flexibilization of production systems. One measure for making production systems more flexible that has been discussed and analyzed in many different ways is the use of automated guided vehicles for material supply within a factory. These are suitable because they meet the five criteria of transformation capability and thus ensure the adaptability of intralogistics [12, 13]. These criteria are universality, mobility, scalability, modularity and compatibility [14]. Against the background of the desired increase in energy efficiency, it is of interest to examine not only the contribution of automated guided vehicles to flexibilization but also their energy consumption structures. Thus, it is possible to consider the energy consumption in the context of production planning and consequently raises the energy efficiency of the production system.

Current considerations of automated guided vehicles focus in particular on their flexibility, whereby energy requirements are often not taken into account. In [15] and [16], for example, it is examined how many automated guided vehicles are required for a production system. In [17] an optimization is presented how automated guided vehicles can perform their tasks in production planning as efficiently as possible. The path finding or optimization of automated guided vehicles motion sequences has also been investigated, as in [18]. The electrical energy requirement is only considered to a secondary extent. For example, in [19] the battery of an automated guided vehicles is considered in the context of a failure modes effects and criticality analysis (FMECA). However, only whether the battery is empty or not is taken into account. In [20], the electrical energy requirement of an autonomously driving forklift truck is taken into account in order to include it in the route finding process. Therefore, only a constant speed is considered in combination with different payload weights. Effects of acceleration, braking or lifting and lowering of load on the energy demand are not analyzed. The energy requirement in [21] and [22] is also included in the path finding problem. But the energy demand is only represented in a simplified way by means of physical formulas which describe the relation between energy demand and payload weight in a linear correlation. Accordingly, on the one hand strong simplifications take place and on the other hand there is no measuring comparison with reality.

From this literature review the objective results for this work to provide a model that represents the electrical power and energy requirements of automated guided vehicles in more detail. This also gives the opportunity to consider the energy efficiency of the logistics processes. The model allows simulations which are used in production planning and enables adaptive production systems to consider the electrical power consumption in their decisions.

To achieve this objective, Section 2 will first present the necessary basic principles for the meaning of intralogistics in a production system and the structure of automated guided vehicles. Subsequently, Section 3 presents measurement data obtained on the electrical power requirements of an automated guided vehicle. Based on this measurement data, movement modules can be defined which classify the different movement types. These movement modules are subsequently modeled in Section 4. The modeling is done according to general physical laws, so that the model can be parameterized for each type of automated guided vehicle. In Section 5 the power profiles generated by the simulation model are compared to the measurement data to validate the simulation model. Finally, Section 6 summarizes the results of this work and outlines further research topics.

2 Basics

In the following, the basics of intralogistics are first presented in Section 2.1 to show why it is of interest to raise efficiency and flexibility. Subsequently, Section 2.2 presents the structure of automated guided vehicles.

2.1 Intralogistic

The objective of logistics is to realize just-in-time production. This means that the correct materials and goods, in the correct quantity, must be in the required place at the specified time with the correct quality [23]. Corporate logistics consists of four fields, as shown in Fig. 1. Acquisition logistics considers the external procurement of resources. Intralogistics focuses on the flow of materials within the factory and thus includes the supply of materials to the individual production processes or their operating resources. Subsequent distribution logistics deals with the delivery of products to the customer. The product cycle is closed by the concluding waste disposal logistics [24, 25].

To increase productivity and efficiency, it is of interest to enhance the complete corporate logistics. Special focus

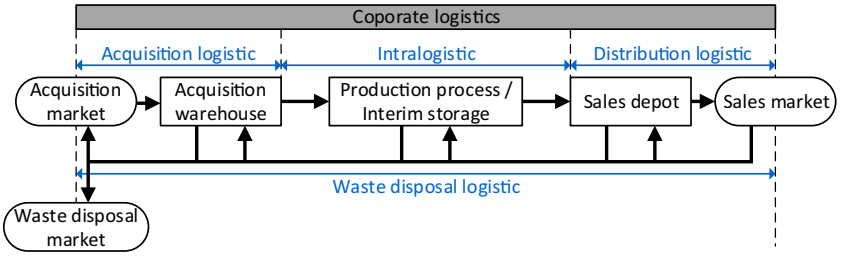

Fig. 1 Corporate logistic with its subfields

in this work is on intralogistics. These comprises the organization, control, implementation and optimization of the internal material flow. Therefore, all logistical material and product flows within a factory site are considered [23–25]. Figure 2 explains how improvements in intralogistics affect the market value V of a product in relation to the costs C. The execution of two production processes $PP1$ and $PP2$ is examined as an example. In the case of a non-optimized intralogistic, there is a waiting time T_{W} before each of the two production processes, which, in addition to the distribution time T_{D} and the processing times T_{PP}, results in the lead time $T_{\mathrm{Production}}$ and the costs $C_{\mathrm{Production}}$. If the intralogistics is improved, the two waiting times are eliminated and the lead time T_{Logistic} is significantly lower. However, the costs increase to $C_{\mathrm{Logistics}}$ because intralogistics becomes more expensive. At the same time, however, the market price will rise to $V_{\mathrm{Logistics}}$, assuming that customers are willing to pay more for faster delivery. The input costs C_{Input} are identical for both variants, since the acquisition of the material is independent of the intralogistical processes [26].

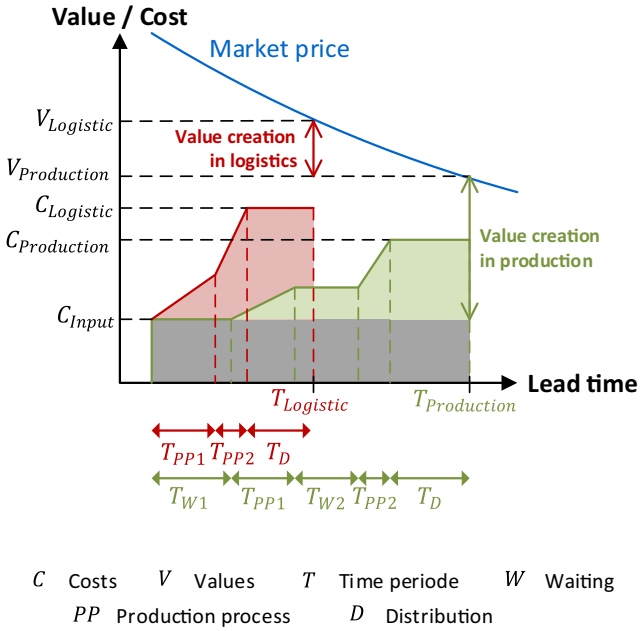

Fig. 2 Value enhancement of production by improved logistics (in reference to [26])

For this reason, the improvement of intralogistics and the associated reduction of lead times is of relevance to companies. Equally important is the flexibilization of production systems. With regard to intralogistics, automated guided vehicles offer the possibility of increasing efficiency and flexibility, which is why they are discussed in more detail below.

2.2 Automated guided vehicles

The development of automated guided vehicle systems (AGVS) began in the USA in the 1950s [27]. The objective of the development was to economize on personnel and improve the material flow [28]. Today an AGVS is defined according to the Association of German Engineers (VDI) by the norm VDI 2510 as an internal, floor-bound transport system with automatically controlled vehicles for material transport. However, this does not involve the transport of employees [29]. Derived from this, an automated guided vehicle (AGV) is an operating resource for material transport and is classically managed by a control system.

The designs of AGVs can be categorized into load-pulling and load-carrying vehicles. Load-carrying AGVs are equipped with a load-carrying device. This allows them to pick up objects from the ground or from a certain height. An example of such a device is an autonomous forklift truck. Load-pulling AGVs can be further divided into two sub-categories. Trailer vehicles pull the material to be transported behind them using a coupling. Underride vehicles, on the other hand, underrun the material to be transported and lift it slightly for the drive [23, 29]. For the measurements and analyses of the electrical power requirement presented in Section 3, an underride vehicle as AGV is considered.

Figure 3 shows the structure of an AGV with special focus on electrical power distribution. The power requirements of an AGV are determined in particular by the embedded-PC, the microcontroller, the sensors and the motors. The microcontroller handles low-level controls, such as the direct control of the motors and the query of measured values from the sensors. At the same time it offers a programming interface for the embedded-PC. This has a better computational capability and is suitable for high-level control, such as motion planning and coordination [30]. The

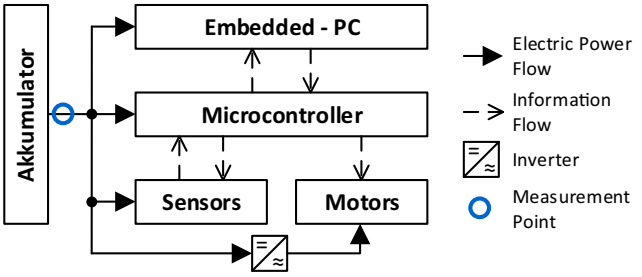

Fig. 3 Typical architecture of an automated guided vehicle in terms of the electrical power distribution (in reference to [30])

components mentioned so far are electrical loads which are supplied by the accumulator. Nowadays, this is typically a lithium-ion battery, as these batteries have a high power density and at the same time a very high energy density [27, 31].

With regard to the coupling of the accumulator and the motors, it must be considered that the battery provides direct current and voltage. For the motors, this must be converted into alternating current and voltage by means of a DC/AC converter. By using an inverter, the motor can also be controlled by pulse width modulation. In this way the speed of the rotor is controlled via the stator frequency of the motor and the speed of the AGV can be adjusted [32–35]. For the electrical power measurements carried out in Section 3, the output direct currents and output direct voltages of the accumulator are measured as marked in Fig. 3.

Typically, AGVs are operated using differential drives. These are characterized by two wheels on the same axis that are powered separately, which controls speed and direction. Figure 4 shows the resulting movements of an AGV as a function of the speed of the left wheel v_l and the right wheel v_r. The speed of the AGV can be specified for both the translational speed v and the angular speed ω depending on the two wheel speeds as

$$v = \frac{v_\mathrm{r} + v_\mathrm{l}}{2} \tag{1}$$

$$\omega = \frac{v_\mathrm{r} + v_\mathrm{l}}{l_\mathrm{AGV}} \tag{2}$$

whereby l_AGV the gauge of the AGV is. Furthermore, the rotational speed of the AGV can be converted by

$$v = \frac{\omega}{\frac{1}{2} \cdot l_\mathrm{AGV}} \tag{3}$$

into a translatory speed.

3 Experimental movement modules determination

The robot *RB1 Base* of the company *Robotnik* is used for the experimental determination of the electrical power requirements of an automated guided vehicle (AGV). This is an underride vehicle which uses a lifting platform to elevate a rack with the material to be transported. For this, the material must be packed in so-called small load carriers. The rack has a weight of 12.5 kg and the small load carrier *R-KLT 6422* has a weight of 2.565 kg. The *RB1 Base* is equipped with two 250-W servo motors. It also has an integrated PC with an Intel i7 processor of the fourth generation, a main memory of 8 GB and a hard disk capacity of 120 GB. The lithium-iron-phosphate accumulator has a nominal capacity of $Q_\mathrm{Akku} = 30$ Ah and a nominal voltage of $U_\mathrm{Akku,nom} = 24$ V, thus realizing a running time of 10 h. Further properties of the *RB1 Base* are listed in Table 1 [36, 37].

To determine the electrical power requirement, the output voltage U_Akku and the output current I_Akku of the accumulator are measured as marked in Fig. 3. Afterwards, the electrical power $P_\mathrm{AGV,el}$ is calculated according to

$$P_\mathrm{AGV,el} = U_\mathrm{Akku} \cdot I_{Akku}. \tag{4}$$

The measurement setup shown in Fig. 5 is applied for this purpose. The *FLUKE 435*$^{Series\ II}$ *Power Quality and Energy Analyzer* is utilized as the measuring instrument and the *HZ O50 Rohde & Schwarz* is utilized as the current clamp to measure the direct current.

The objective of the experiments is to identify movement modules with respect to the electrical power consumption of the AGV. These movement modules are classified into the translatory movement, the rotary movement, and the lifting and lowering movement of the platform. Thereby

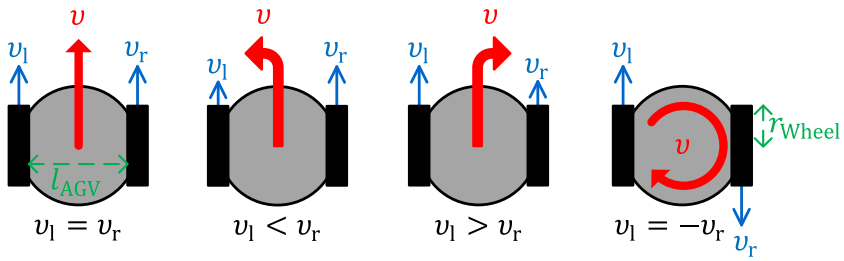

Fig. 4 Movements of an AGV with differential drive

Table 1 Technical characteristics of the *RB1 Base* automated guided vehicle from *Robotnik* [36, 37]

Characteristic	Symbol	Value
Wheel radius	r_{Wheel}	0.0762 m
Gauge	l_{AGV}	0.421 m
Own weight	m_{AGV}	30 kg
Maximum payload	$m_{\text{Load,max}}$	50 kg
Translation speed limit	υ_{max}	1.5 m/s
Rotational speed limit	ω_{max}	3 rad/s
Translation maximum acceleration	a_{max}	1.5 m/s^2
Translation minimum acceleration	a_{min}	−0.68 m/s^2
Rotational maximum acceleration	α_{max}	3 rad/s^2
Lifting distance	s_{Lift}	0.035 m
Lifting time	t_{Lift}	6.5 s
Lifting speed	υ_{Lift}	0.005 m/s
Lifting acceleration	a_{Lift}	0.01 m/s^2

different translatory speeds υ, rotational speeds ω and payload weights m_{Load} have to be considered.

The payload weight m_{Load} is varied from 2.05 up to 48.125 kg in 10.34-kg steps. The payload weight of 2.05 kg corresponds to an empty run without a rack, so that only the measuring equipment is carried along. The translatory speed υ and is changed in steps of 0.3 m/s whereby the lowest speed is 0.6 m/s and the maximum speed is 1.5 m/s. To analyze the translatory movement a distance s of 20 m is chosen to perform the experiments. The rotatory speed ω is varied between 1.2 rad/s and 3 rad/s with a step size of 0.6 rad/s. Thereby, only 90° and 180° rotations β are examined. Accordingly, this involves turning the AGV or reversing it. In addition there are 4 experiments each for lifting respectively lowering the different payloads. The combination of these parameters results in 68 experiments,

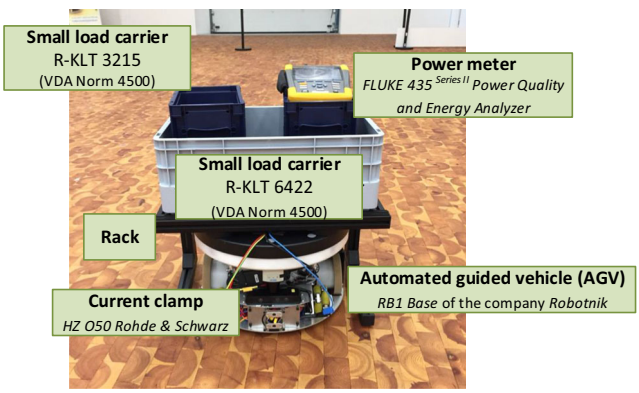

Fig. 5 Measurement setup to analyze the electrical power and energy consumption of the automated guided vehicle *RB1 Base*

which are carried out to determine the movement modules of the AGV. The execution of the individual movements is manually operated by a controller. In order to eliminate fluctuations that occur, each of the experiments is performed ten times and an average mean value is determined from the respective measurement data.

As an example, Fig. 6 shows the recorded measurement data of the translatory movement over 20 m with a speed of 1.2 m/s and a payload weight of 2.05 kg. These measurement data are then averaged, resulting in the electrical power profile in Fig. 7. In the following subsections, the presentation of the actual measurement data is omitted and the averaged power profiles are presented directly.

For the following analyses and also the modeling implemented in Section 4, it must be considered that only one type of AGV was used for the experimental investigations. Consequently, other types, such as load-carrying AGVs (for example, autonomous forklift trucks), may result in different movement modules. Similarly, the power and energy requirements shown in the following refer only to the *RB1 Base*. Therefore, it must also be taken into account that other underride vehicles have different power and energy requirements.

3.1 Translatory movement module

Figure 8 shows the three identified movement modules for translatory movement regarding the electrical power consumption $P_{\text{AGV,el}}$. These are *Acceleration*, *Rolling* at constant speed and finally *Braking* to a standstill. For braking, it must be considered that negative power may occur for individual runs. This power can generally be used for recuperation in order to recharge the accumulator.

Next, Fig. 9 shows the influence of the payload weight m_{Load} of the AGV on its electrical power consumption. It is obvious that an increasing weight has an influence on all three movement modules of the translatory motion. The power demand rises with increasing weight.

Similarly, the speed of the AGV υ has an influence on all three movement modules, as shown in Fig. 10. The speed influences both the electrical power demand and the time required to cover a distance of $s = 20$ m. As the speed increases, the electrical power consumption increases, but the required driving time is reduced.

In order to analyze the relationship between speed and time in terms of its impact on energy efficiency, it is necessary to consider the energy consumption. For this purpose, Fig. 11 shows the respective energy requirements at varying speed and payload weight. It can be seen that an increased payload weight leads to a general rise in the energy consumption, as can be seen from the increasing power in Fig. 9. Furthermore, it can be seen that an increase

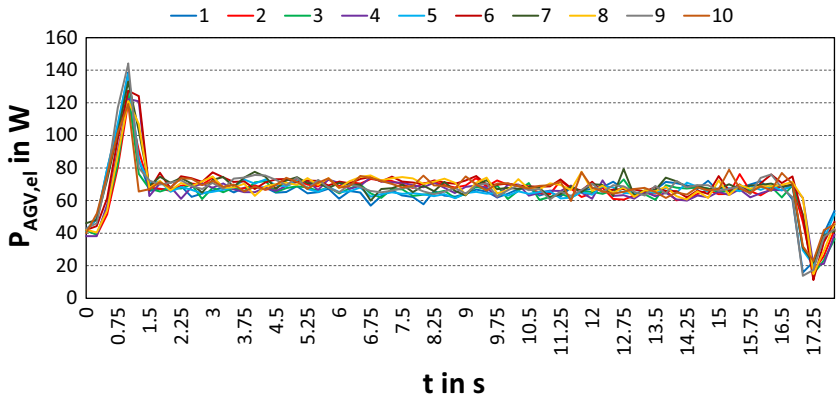

Fig. 6 Measurement data of ten runs regarding the translatory movement ($\upsilon = 1.2\,\mathrm{m/s}$, $m_{\mathrm{Load}} = 2.05\,\mathrm{kg}$, $s = 20\,\mathrm{m}$)

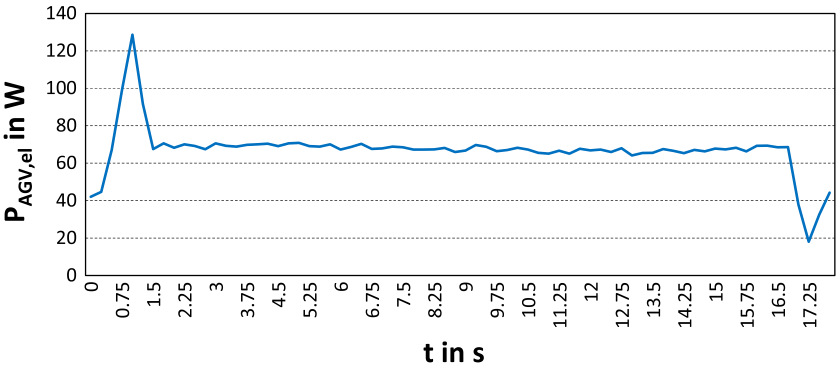

Fig. 7 Average power profile of the translatory movement ($\upsilon = 1.2\,\mathrm{m/s}$, $m_{\mathrm{Load}} = 2.05\,\mathrm{kg}$, $s = 20\,\mathrm{m}$)

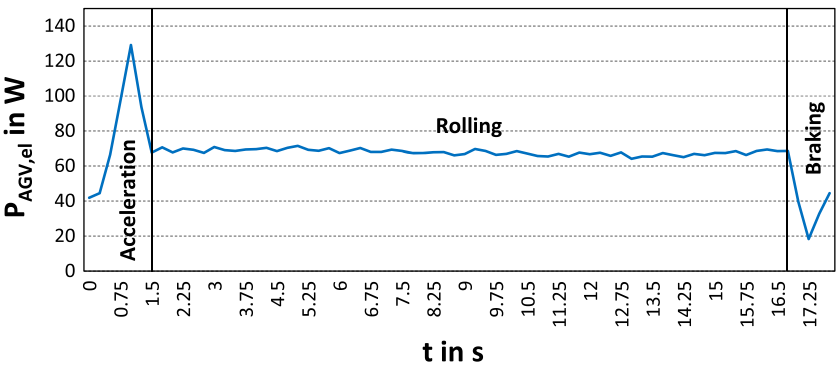

Fig. 8 Movement modules regarding the translatory movement of the AGV ($\upsilon = 1.2\,\mathrm{m/s}$, $m_{\mathrm{Load}} = 2.05\,\mathrm{kg}$, $s = 20\,\mathrm{m}$)

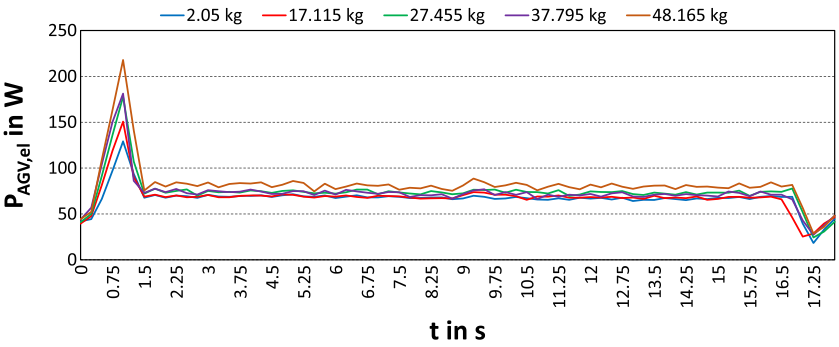

Fig. 9 Influence of the payload weight on the electrical power requirement for the translatory movement ($\upsilon = 1.2\,\mathrm{m/s}$, $m_{\mathrm{Load}} = \{2.05\,kg;\ 17.155\,\mathrm{kg};\ 27.455\,\mathrm{kg};\ 37.795\,\mathrm{kg};\ 48.165\,\mathrm{kg}\}$, $s = 20\,\mathrm{m}$)

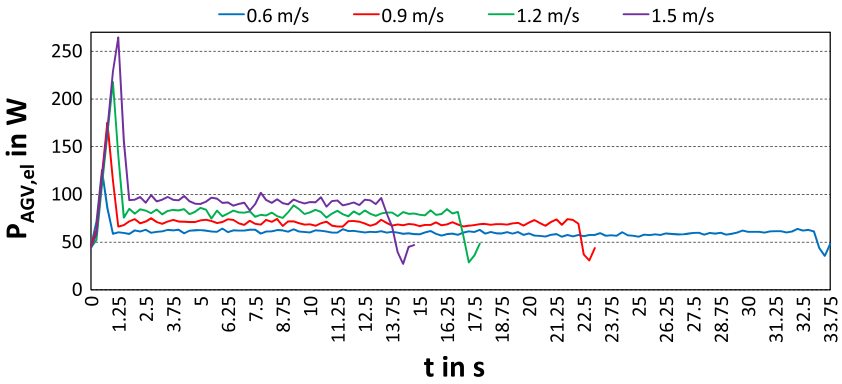

Fig. 10 Influence of the speed on the electrical power requirement for the translatory movement ($\upsilon = \{0.6\,\text{m/s};\ 0.9\,\text{m/s};\ 1.2\,\text{m/s};\ 1.5\,\text{m/s}\}$, $m_{\text{Load}} = 48.165\,\text{kg}$, $s = 20\,\text{m}$)

in speed with constant payload leads to a lower energy requirement. This is mainly due to the shorter driving time. It follows that an AGV is most efficient when it is operating at its maximum speed. Although this leads to an increased power requirement, the energy consumption is reduced by saving driving time as pictured in Fig. 10.

3.2 Rotatory movement module

For the rotation of the AGV, Fig. 12 shows an example of the average power consumption for a rotation of $\beta = 180°$ with a payload of $m_{\text{Load}} = 27.455\,\text{kg}$ and an angular velocity of $\omega = 2.4\,\text{rad/s}$. The three movement modules *Acceleration*, *Rolling* at constant speed and *Braking* to standstill are identified analogous to the translation motion. For rotation, it should be noted that the section of movement at constant speed is significantly shorter than for translational movement. This means that the acceleration and braking portion predominates.

For the influence of the payload weight and the speed on the power requirement of the rotary movement, the result is analogous to the translatory movement. An increased weight leads to an increased power requirement, as Fig. 13 shows. An increasing speed also leads to a rising power requirement, whereby the driving time is also reduced here, as Fig. 14 demonstrates.

Again, the examination of the energy demand in Fig. 15 shows that higher speed leads to reduced energy consumption. Consequently, the highest speed should also be used for the rotation of the AGV for energy efficient operation, analogous to the translatory motion.

With regard to a rotation β of the AGV by 90°, similar results are obtained, which are not described in detail here.

3.3 Lifting and lowering movement module

Lifting or lowering the load is always carried out over a vertical distance of $s_{\text{Lift}} = 0.035\,\text{m}$ at a speed of $\upsilon_{\text{Lift}} = 0.005\,\text{m/s}$. For this reason only the payload weight m_{Load} has an influence on the electrical power requirement $P_{\text{AGV,el}}$ of the AGV. For the payload, the empty weight of 2.05 kg is not investigated because an AGV only carries out a lifting or lowering movement in real operation when a load is on board.

For the lifting of loads, there are five movement modules as shown in Fig. 16. Analogous to the translatory and rotational movement modules, the lifting starts with an *Acceleration* and ends with a *Braking*. After the acceleration, there is a phase in which the lifting platform moves upwards, but does not yet have any contact with the load. This movement module is called *Lifting without load*. Therefore the electric power consumption is comparatively low. Afterwards there is a phase in which the load is elevated from the ground and its movement module is named *Lifting load absorption*. This causes an increase in electrical power. As soon as the load is completely elevated from the ground,

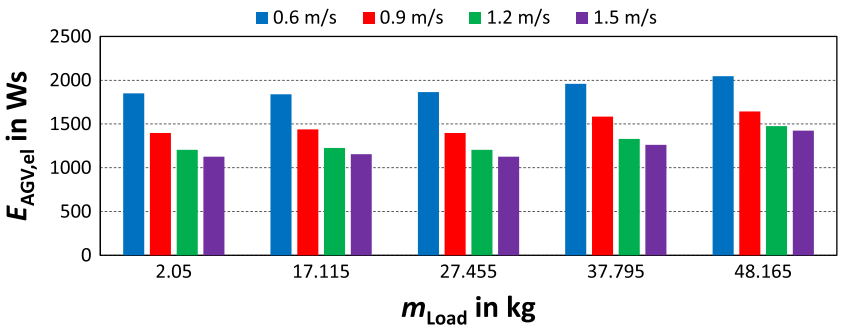

Fig. 11 Energy consumption for the translatory movement depending on the speed ($\upsilon = \{0.6\,\text{m/s};\ 0.9\,\text{m/s};\ 1.2\,\text{m/s};\ 1.5\,\text{m/s}\}$, $m_{\text{Load}} = \{2.05\,kg;\ 17.155\,\text{kg};\ 27.455\,\text{kg};\ 37.795\,\text{kg};\ 48.165\,\text{kg}\}$, $s = 20\,\text{m}$)

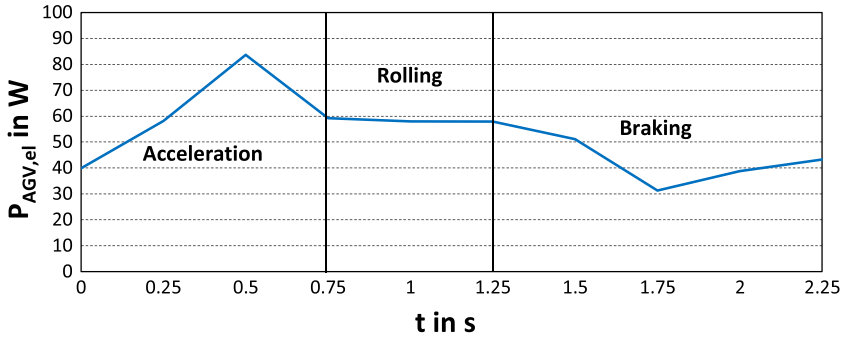

Fig. 12 Movement modules regarding the rotatory movement of the AGV ($\omega = 2.4\,\text{rad/s}$, $m_{\text{Load}} = 27.455\,\text{kg}$, $\beta = 180°$)

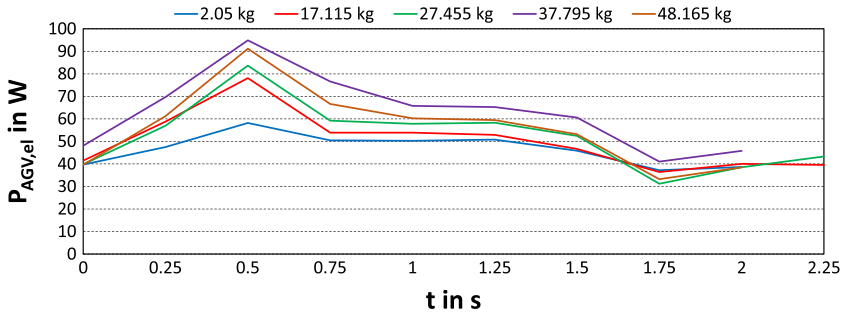

Fig. 13 Influence of the payload on the electrical power requirement for the rotatory movement ($\omega = 2.4\,\text{rad/s}$, $m_{\text{Load}} = \{2.05\,kg;$ $17.155\,\text{kg};\ 27.455\,\text{kg};\ 37.795\,\text{kg};\ 48.165\,\text{kg}\}$, $\beta = 180°$)

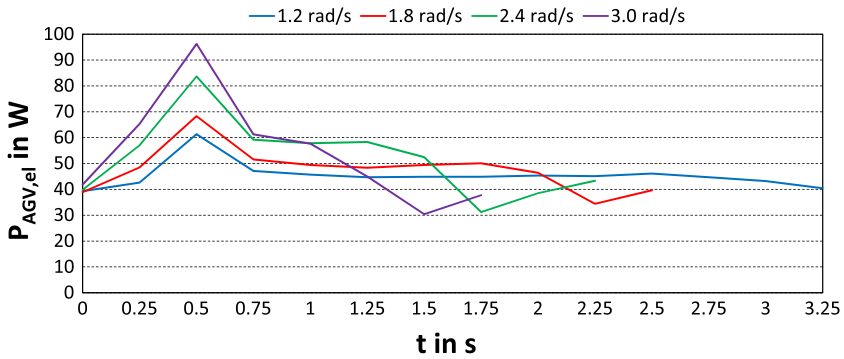

Fig. 14 Influence of the angular speed on the electrical power requirement for the rotatory movement ($\omega = \{1.2\,\text{rad/s};\ 1.8\,\text{rad/s};\ 2.4\,\text{rad/s};\ 3.0\,\text{rad/s}\}$, $m_{\text{Load}} = 27.455$, $\beta = 180°$)

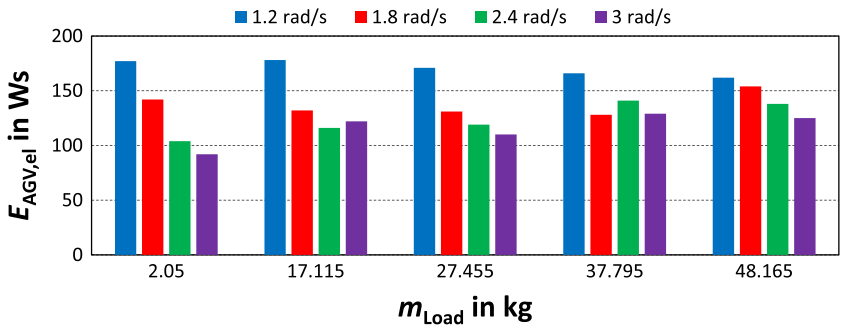

Fig. 15 Energy consumption for the rotatory movement depending on the speed and payload ($\omega = \{1.2\,\text{rad/s};\ 1.8\,\text{rad/s};\ 2.4\,\text{rad/s};\ 3.0\,\text{rad/s}\}$, $m_{\text{Load}} = \{2.05\,kg;\ 17.155\,\text{kg};$ $27.455\,\text{kg};\ 37.795\,\text{kg};\ 48.165\,\text{kg}\}$, $\beta = 180°$)

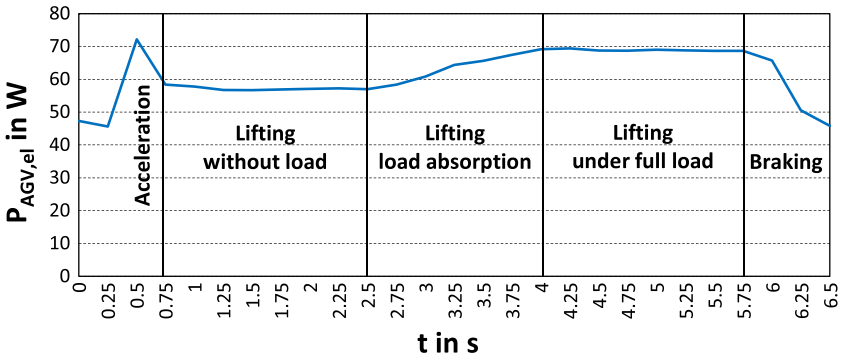

Fig. 16 Movement modules regarding the lifting of payload ($\upsilon_{\text{Lift}} = 0.005\,\text{m/s}$, $m_{\text{Load}} = 27.455\,\text{kg}$, $s_{\text{Lift}} = 0.035\,\text{m}$)

Lifting under full load takes place with a comparatively high power consumption.

Figure 17 shows the influence of the payload weight for lifting on the electrical power requirement of the motor. It can be seen that an effect only occurs when the lifting platform gets in contact with the load. Then the higher the payload, the more power the AGV requires.

A similar power behavior is obtained for lowering the load, as shown in Fig. 18. Here the phases of *Lowering under full load* and *Lowering without load* are interchanged in relation to lifting. In addition, there is a decrease in power consumption from the moment the load touches the ground which is described by the movement module *Lowering load discharge*.

In addition, Fig. 19 shows the influence of the payload weight on the power requirement. It can be seen that the weight has an influence on the movement modules *Acceleration*, *Lowering under full load* and *Lowering load discharge*. The movement modules *Lowering without load* and *Braking*, however, are independent of the load weight.

The investigation of the energy requirement in Fig. 20 shows an increasing energy demand for both lifting and lowering in relation to the rising payload weight. Since the speed cannot be varied in this case, it has no influence on the energy consumption and thus on the energy efficiency.

4 Modeling of the movement modules

In order to enable the identified movement modules to be used for each type of automated guided vehicle (AGV), they are modeled. So, simulations of the electrical energy requirements of AGVs can be performed and considered in production planning. But the model presented in the following is only valid for underride vehicles which have the same movement modules as the *RB1 Base* which is analyzed in the previous section. The objective is that the implementation can be parameterized depending on the technical characteristics of an AGV. For this reason general physical laws are used so that the simulation model can be adapted to similar AGVs in relation to the *RB1 Base*. This is also the reason why no data driven simulation approach is chosen, although the necessary measurement data are available. For other types of AGVs, such as load-carrying vehicles, this simulation model is not adaptable or parameterizable. This requires the development of an individual simulation model.

As already in the context of data acquisition, the modeling also focuses on the motors of the AGV. The total electrical power $P_{\text{AGV,el}}$ is composed as

$$P_{\text{AGV,el}}(t) = P_{\text{Motor,el}}(t) + P_{\text{Support,el}}. \tag{5}$$

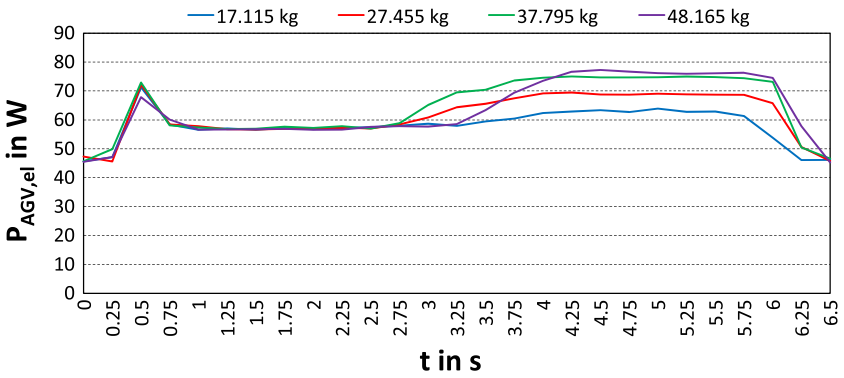

Fig. 17 Influence of the payload weight on the electrical power requirement for lifting the load ($\upsilon_{\text{Lift}} = 0.005\,\text{m/s}$, $m_{\text{Load}} = \{17.155\,\text{kg};\ 27.455\,\text{kg};\ 37.795\,\text{kg};\ 48.165\,\text{kg}\}$, $s_{\text{Lift}} = 0.035\,\text{m}$)

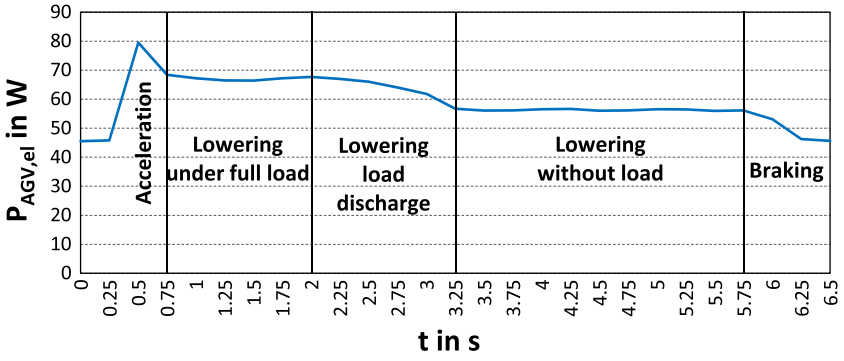

Fig. 18 Movement modules regarding the lowering of payload ($\upsilon_{\text{Lift}} = 0.005\,\text{m/s}$, $m_{\text{Load}} = 48.165\,\text{kg}$, $s_{\text{Lift}} = 0.035\,\text{m}$)

The support power $P_{\text{Support,el}}$ comprises the electrical power consumption of the embedded-PC, the microcontroller and the sensors. The required support power can be measured while the AGV is idling. For the robot *RB1 Base* applied here the support power is $P_{\text{Support,el}} = 43.27\,\text{W}$. In relation to a maximum measured power value of 95 W during operation (neglecting acceleration movements), the support power takes up a high share of the power requirement.

When considering the electrical power $P_{\text{Motor,el}}(t)$ of the motor, the necessary mechanical power $P_{\text{Motor,mech}}(t)$ must be taken into account on the one hand, and the efficiency of the motor η_{Motor} and the inverter η_{Inverter} on the other. The electrical power of the motor is therefore calculated as

$$P_{\text{Motor,el}}(t) = P_{\text{Motor,mech}}(t) \cdot \frac{1}{\eta_{\text{Motor}}} \cdot \frac{1}{\eta_{\text{Inverter}}} \tag{6}$$

A value of 0.96 can generally be assumed for the efficiency of the inverters [38]. However, electric motors with a rated power of 250 W usually have significantly lower efficiency. Therefore a rate of 0.625 is assumed here [39]. In order to model the mechanical motor power $P_{\text{Motor,mech}}(t)$ as a function of the movements of the AGV, the different movement modules are considered in the following Sections 4.1, 4.2 and 4.3. The modeling of the individual movements by physical laws is used in Section 4.4 to implement state flow graphs.

4.1 Modeling translatory movement module

The mechanical power $P_{\text{trans,mech}}$ of the translatory movement is generally expressed by

$$P_{\text{trans,mech}} = \vec{F} \cdot \vec{\upsilon}_{\text{F}} \tag{7}$$

as a function of the force $\vec{F}$ and the speed $\vec{\upsilon}_{\text{F}}$ of the object. For the consideration of an AGV, the driving resistance F_{DR} can be used, which is composed of the air resistance, rolling friction resistance F_{RF}, gradient resistance and acceleration resistance F_{AR}. Due to the low maximum speed of the AGV of 1.5 m/s, the air resistance can be neglected. Gradient resistance is also neglected, since factory buildings usually have no gradient. Consequently, the mechanical power of the translatory movement is

$$P_{\text{trans,mech}}(t) = F_{\text{DR}} \cdot \upsilon(t) = (F_{\text{RF}} + F_{\text{AR}}) \cdot \upsilon(t). \tag{8}$$

The rolling resistance occurs due to the deformation work of the wheels at the contact points with the floor and is calculated as

$$F_{\text{RF}} = \mu_{\text{RF}} \cdot (m_{\text{AGV}} + m_{\text{Load}}) \cdot g \tag{9}$$

depending on the own weight of the AGV m_{AGV}, its payload m_{Load} and the gravitational acceleration $g = 9.81\,\text{m/s}^2$. The rolling resistance coefficient μ_{RF} depends on the material properties of the floor and wheels. This coefficient is determined by the measurement data obtained from the experiment in the previous section. This results in a value

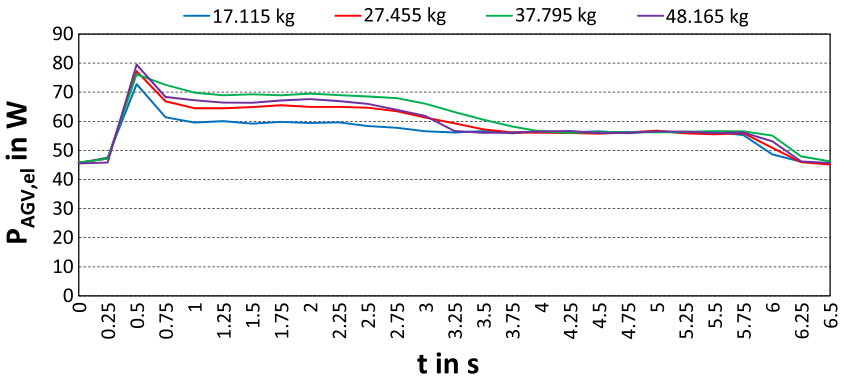

Fig. 19 Influence of the payload weight on the electrical power requirement for lowering the load ($\upsilon_{\text{Lift}} = 0.005\,\text{m/s}$, $m_{\text{Load}} = \{17.155\,\text{kg};\ 27.455\,\text{kg};\ 37.795\,\text{kg};\ 48.165\,\text{kg}\}$, $s_{\text{Lift}} = 0.035\,\text{m}$)

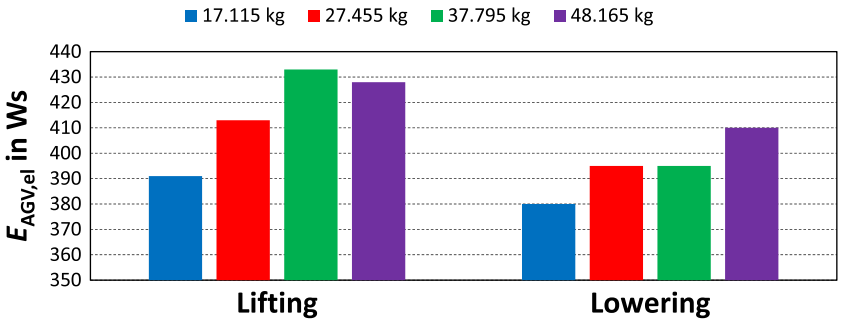

Fig. 20 Energy consumption of the lifting and lowering depending on the different payloads ($\upsilon_{Lift} = 0.005\,m/s$, $m_{Load} = \{17.155\,kg;\ 27.455\,kg;\ 37.795\,kg;\ 48.165\,kg\}$, $s_{Lift} = 0.035\,m$)

of $\mu_{RF} = 0.0265$ which is a typical parameter for AGVs in relation to [40].

The acceleration resistance F_{AR} can be determined using Newton's 2nd law according to

$$F_{AR} = (m_{AGV} + m_{Load}) \cdot a(t). \tag{10}$$

Regarding the three movement modules for the translatory motion, a case distinction must be made for the acceleration of the AGV:

$$a(t) = \begin{cases} a_0 + \mu_{RF} \cdot g, & if\ a(t) > 0\ \text{(Acceleration)} \\ 0, & if\ a(t) = 0\ \text{(Rolling)} \\ a_0 - \mu_{RF} \cdot g, & if\ a(t) < 0\ \text{(Braking)} \end{cases} \tag{11}$$

The measurements have shown a maximum acceleration of $a_{max} = 1.5\,m/s^2$ for the *RB1 Base*, so $a_0 = a_{max} = 1.5\,m/s^2$ is set here.

For the mechanical power of the translatory movement, the following results can be combined

$$P_{trans,mech} = (m_{AGV} + m_{Load}) \cdot (\mu_{RF} \cdot g + a(t)) \cdot \upsilon(t) \tag{12}$$

and used within the simulation model to represent the mechanical power. By means of Eq. (6), the electrical power required for the translatory movement through the accumulator of the AGV can then be calculated.

4.2 Modeling rotatory movement module

For the modeling of the mechanical power for the rotation of the AGV, starting from

$$P_{rot,mech} = \vec{M} \cdot \vec{\omega}, \tag{13}$$

an analogous approach to that previously used for translational motion can be applied. The following relationship results for the torque M in dependence of the rolling friction resistance and the acceleration resistance:

$$M = \frac{F_{RF}+F_{AR}}{2} \cdot l_{AGV} = (m_{AGV} + m_{Load}) \cdot (\mu_{RF} \cdot g + a(t)) \cdot \upsilon(t) \tag{14}$$

This results for the mechanical rotational power in

$$P_{rot,mech} = (F_{RF} + F_{AR}) \cdot \frac{l_{AGV}}{2} \cdot \omega(t) = (m_{AGV} + m_{Load}) \cdot (\mu_{RF} \cdot g + a(t)) \cdot \frac{l_{AGV}}{2} \cdot \omega(t) \tag{15}$$

4.3 Modeling lifting and lowering movement module

The lifting and lowering movement is performed by means of a spindle drive. This is a movable screw which generates a vertical linear movement from the rotational movement of the motor [41]. The electrical stationary spindle power $P_{stat,Spin,el}$ is given by

$$P_{stat,Spin,el} = \frac{M_L \cdot n}{9.55} \cdot \frac{1}{\eta_{Spin}}. \tag{16}$$

Accordingly, the stationary spindle power is dependent on the load torque M_L, the spindle speed n and the efficiency of the spindle η_{Spin} [42]. It is assumed that a 1-gear trapezoidal gearbox is the spindle drive. Therefore, an efficiency of $\eta_{Spin} = 0.13$ is assumed, since there is a high friction loss between the spindle nut and the thread [43].

The load torque can be calculated as

$$M_L = \frac{h_{Spin}}{2 \cdot \pi} \cdot (F_G + F_{Feed}). \tag{17}$$

The spindle pitch h_{Spin} for the *RB1 Base* corresponds to a height of 0.005 m. For the gravity force F_G it must be taken into account that only the weight of the lifting platform including the spindle drive $m_{Platform} = 3\,kg$ and the payload weight m_{Load} are lifted [42].

To determine the spindle speed n, the following two relationships can be used.

$$\omega = \frac{2 \cdot \pi \cdot \upsilon(t)}{h_{Spin}} \tag{18}$$

$$\omega = \frac{2 \cdot \pi \cdot n(t)}{60} \tag{19}$$

Equating Eqs. (18) and (19) results in

$$n(t) = \frac{\upsilon(t) \cdot 60}{h_{Spin}} \tag{20}$$

for the spindle speed [41]. Since the lifting and lowering movement always covers a distance of $s_{Lift} = 0.035\,m$ and always requires a time of $t_{Lift} = 6.5\,s$, the spindle speed υ_{Lift} can be set to 0.005 m/s.

Table 2 Assumed parameter values for the power consumption of the spindle drive from [43]

Parameter	Symbol	Value
Feed process force	F_{Feed}	350 N
Weight of the platform	m_{Platform}	3 kg
Spindle pitch	h_{Spin}	0.005 m
Efficiency of the spindle	η_{Spin}	0.13

In summary, this results in the stationary electrical power consumption of the spindle to

$$P_{\text{stat,Spin,el}} = \frac{h_{\text{Spin}}}{2 \cdot \pi} \cdot (F_{\text{g}} + F_{\text{Feed}}) \cdot n(t) \cdot \frac{1}{\eta_{\text{Spin}}}. \tag{21}$$

The parameters listed in Table 2 are applied to model the spindle power of the automated guided vehicle *RB1 Base* which is used here as application example.

For a complete description of the power requirement of the spindle, the acceleration moment M_{A} resulting after

$$M_{\text{A}} = \frac{J_{\text{Spin}} \cdot n}{t_{\text{A}} \cdot 9.55} \tag{22}$$

would also have to be taken into account [41]. However, the necessary data for determining the mass moment of inertia J_{Spin} are not available. Therefore, the modeling is only carried out as a function of the stationary power consumption.

4.4 State flow graphs

The preceding physical modeling of the individual movement modules is implemented in the following as a state flow graph. This procedure has the superordinate objective of realizing an event-discrete simulation. The background to this is that many factory simulations are implemented as such event-discrete simulations [44–47]. The software tool Matlab/Simulink is used here.

Figure 21 presents the state flow graph for the translatory motion. This graph can be used analogue for the rotational movement, only the corresponding parameters for the rotation have to be applied. For modeling, a so-called superstate is used, which has four substates in the case of translational or rotational motion. These substates correspond to the three movement modules identified in Sections 3.1 and 3.2. Additionally, the idle state is implemented.

As input variables, the superstate requires the desired speed υ_{set} of the AGV. For example, this speed can originate from a higher-level factory control system that instructs the AGV which task has to be performed with which parameters (distance, speed, etc.). Previous analyses in Section 3 have shown that an AGV is most energy efficient when it operates at maximum speed $\upsilon_{\text{max}} = 1.5$ m/s. In addition, the distance s of the transport order is required. Furthermore, the message {*EntityArrives*} is required as an interface between the state graph and the event-discrete simulation model of a production line. Additional variables that describe the technical characteristics of the AGV, such as maximum acceleration a_{max} or minimum acceleration a_{min} or own weight m_{AGV}, must be stored within the state graph.

As soon as the AGV has to execute a transport, the message {*EntityArrives*} reaches the state flow graph and the idle substate is left. This starts the acceleration of the AGV. The processing of the substates can be controlled by the acceleration $a(t)$. In this way, the AGV leaves the acceleration state as soon as the set speed υ_{set} is reached. The speed $\upsilon(t)$ results from the integration of the acceleration. The rolling state is executed until the desired transport distance s is reached. This results from the double integration of the acceleration. However, the braking distance s_{Braking} of the AGV must be considered

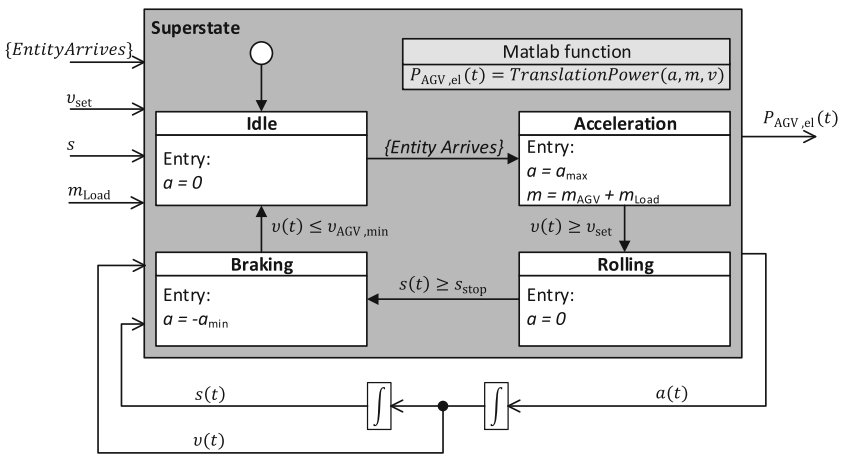

Fig. 21 State flow graph for the transaltory movement

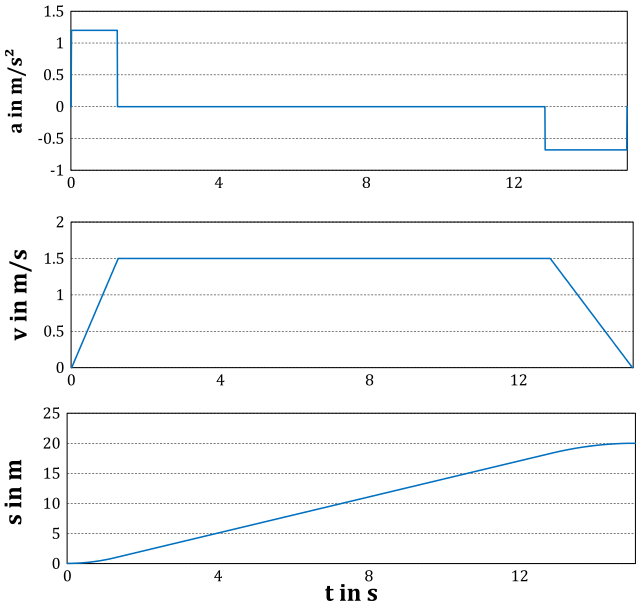

Fig. 22 Simulation results for the acceleration a, speed υ and distance s for the translatory movement

and subtracted from the transport distance s. Hence the distance s_{stop} is given as

$$s_{\text{stop}} = s - s_{\text{Braking}} = s - \frac{\upsilon_{\text{set}}^2}{2 \cdot a_{\text{min}}}. \tag{23}$$

An exemplary course for the acceleration a and the resulting speed υ of the AGV respectively the distance s covered is shown in Fig. 22.

The electrical power requirement $P_{\text{AGV,el}}(t)$ is calculated within the superstate using a Matlab function depending on acceleration a, total mass m and speed υ. The physical laws described above are applied for this purpose.

Figure 23 shows the corresponding state flow graph for the lifting movement. By switching the two states *Lifting without load* and *Lifting under full load*, the state graph for the lowering movement of the AGV can be realized.

Since the lifting and lowering movements are predefined motion sequences that vary neither in their lifting distance nor their temporal duration, the processing of the substates is always the same. For this reason, the implementation is carried out by the *after(Time)* function depending on the measured times for the separate movement modules. Accordingly, the state graph only requires the payload weight m_{Load} as input variable and the message {*EntityArrives*}. This message starts a lifting or lowering movement, for example when the AGV has arrived at its destination and should pick up a load there. The technical characteristics of the modeled AGV must also be stored here in the state graph, such as the weight of the platform m_{Platform} or the acceleration of the lifting movement a_{Lift}.

Once again, the resulting electrical power $P_{\text{AGV,el}}$ is calculated as an output variable using a Matlab function within the superstate. Within the Matlab function, the physical equations from Section 4.3 are implemented respectively.

The presented implementation of the electrical power requirements of AGVs can also be adapted to other models by parameterization. It should be noted that the *RB1 Base* application example is an underride vehicle. If a different type of AGV should be simulated, the state graphs must be adapted accordingly. For the parameterization of the state graphs, the corresponding technical characteristics of the AGV that is to be modeled must be known. These include, for example, the minimum and maximum acceleration or the own weight. But also properties of the operating site must be taken into account, for example to determine the rolling resistance.

Fig. 23 State flow graph for the lifting movement

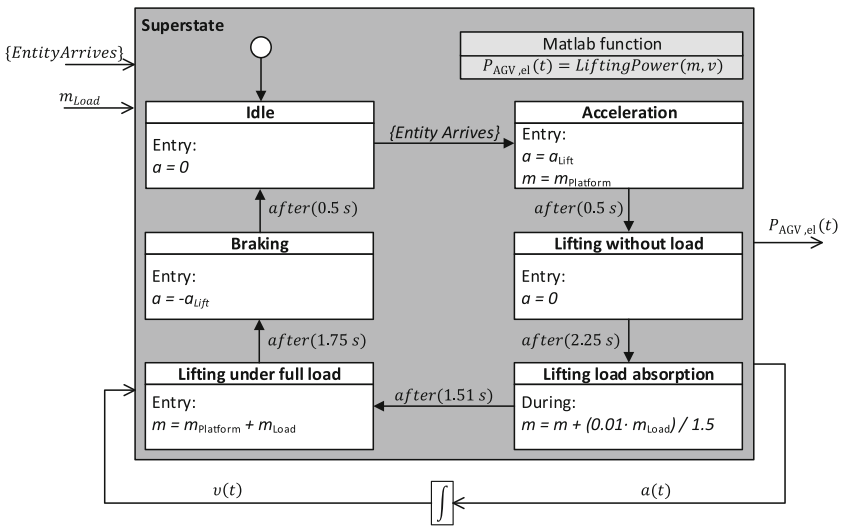

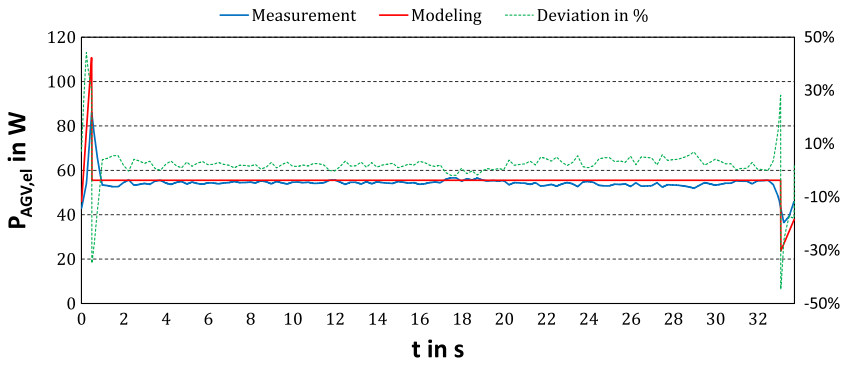

Fig. 24 Comparison between the measured values and the simulated values regarding the electrical power of the translatory movement ($\upsilon = 0.6\,\mathrm{m/s}$, $m_{\mathrm{Load}} = 17.115\,\mathrm{kg}$, $s = 20\,\mathrm{m}$)

5 Validation of the model

The following Figs. 24, 25, 26 and 27 present the comparison between the recorded measured values and the simulated values of the electrical power demand of the *RB1 Base* as an automated guided vehicle (AGV). To compare the recorded measured values with the results of the simulation, the percentage deviation is utilized. The percentage deviation of the electrical power is determined according to

$$\Delta P = \frac{P_{\mathrm{Modeling}} - P_{\mathrm{Measurement}}}{P_{\mathrm{Measurement}}} \cdot 100\%. \tag{24}$$

This results in a deviation between the modeled and measured power values for each point in time. Analogously, the energetic deviation according to

$$\Delta E = \frac{E_{\mathrm{Modeling}} - E_{\mathrm{Measurement}}}{E_{\mathrm{Measurement}}} \cdot 100\% \tag{25}$$

is also determined for each movement module. Thereby, not each single point of time is considered, but the execution of a complete movement, i.e. a complete translatory, rotational as well as lifting or lowering movement.

Figure 24 shows the comparison for the translatory movement. Especially for the movement with constant speed there are nearly no deviations. This is also evident for the remaining combinations of payload weight and speed. With regard to acceleration and braking, the amplitude deviations are particularly noticeable. The arithmetic mean value of the power deviation in percent for the pictured translatory movement is $\Delta\overline{P} = 2.15\%$. For the energetic evaluation of the translatory motion, a modeled energy requirement of $E_{\mathrm{Modeling}} = 1737\,\mathrm{Ws}$ results. This is compared to a measured energy consumption of $E_{\mathrm{Measurement}} = 1840\,\mathrm{Ws}$, resulting in a deviation of $\Delta E = -5.59\%$.

Next, Fig. 25 shows the two power curves for the rotary motion of the AGV. Here an average deviation of $\Delta\overline{P} = 7.17\%$ results. There are larger deviations for the accelerations and brakes in relation to the rotation at constant speed. Shown here is the maximum rotation speed with maximum load. For lower speeds and loads there are smaller deviations. But also for low speeds and loads there are significant deviations in the dynamic movements of acceleration and braking. The higher the speed of the rotation, the shorter the movement module rotation at constant speed becomes, resulting in greater deviations between the modeled and measured performance profiles. A further problem results from the total time duration of the 180° rotation, which only lasts 1.75 s. Since the measuring device provides values with a temporal resolution of 0.25 s, the comparison is based on only 9 separate measured values. These differences are consequently also apparent in the energy perspective. An energy of $E_{\mathrm{Measurement}} = 125\,\mathrm{Ws}$ is measured for this rotation, while the model displays a reduced energy requirement of $E_{\mathrm{Modeling}} = 101\,\mathrm{Ws}$. This results in a deviation of $\Delta E = -19.2\%$. Due to these

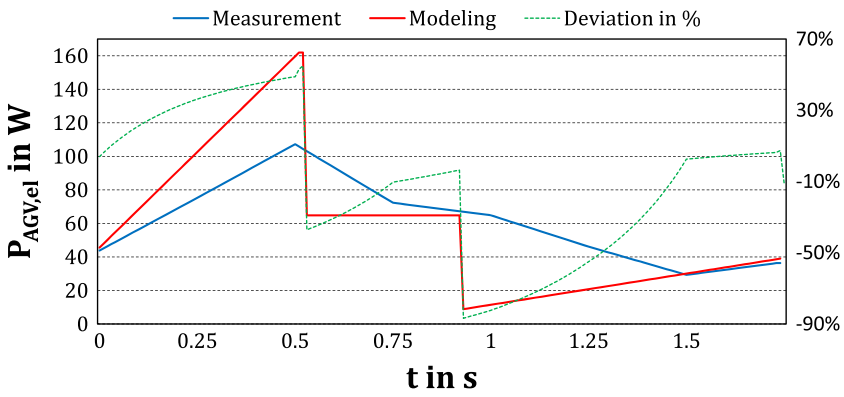

Fig. 25 Comparison between the measured values and the simulated values regarding the electrical power of the rotatory movement ($\omega = 3.0\,\mathrm{rad/s}$, $m_{\mathrm{Load}} = 48.165\,\mathrm{kg}$, $\beta = 180°$)

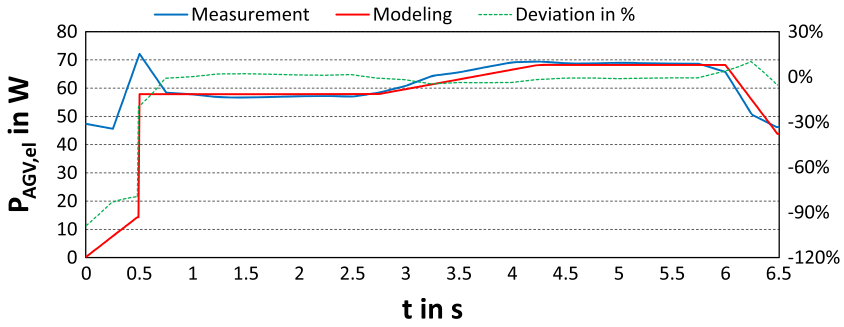

Fig. 26 Comparison between the measured values and the simulated values regarding the electrical power of the lifting movement ($v_{\text{Lift}} = 0.005\,\text{m/s}$, $m_{\text{Load}} = 48.165\,\text{kg}$, $s_{\text{Lift}} = 0.035\,m$)

significant deviations, it will be necessary in the future to model the rotation in more detail and to measure the electrical power in a higher time resolution.

Figure 26 shows the validation results for lifting a load, while Fig. 27 displays the lowering movement. For both modeled power requirements, there are hardly any deviations in the movement modules *Lifting without load*, *Lifting load absorption*, *Lifting under full load*, and *Braking*. However, also here for both movements a clear deviation within the movement module *Acceleration* is shown. The average power deviation for the lifting movement is $\Delta\overline{P} = 5.65\%$ while the deviation for the lowering movement is $\Delta\overline{P} = 7.63\%$. For the lifting movement an electrical energy requirement of $E_{\text{Measurement}} = 398\,\text{Ws}$ is measured, while the simulation gives a value of $E_{\text{Modeling}} = 428\,\text{Ws}$. Hence, there is a deviation of $\Delta E = -7.10\%$. A similar result is obtained for the lowering movement. A deviation of $\Delta E = 3.54\%$ occurs in this case, which is calculated from a measured energy of $E_{\text{Measurement}} = 395\,\text{Ws}$ and a modeled energy of $E_{\text{Modeling}} = 409\,\text{Ws}$.

In summary, it is possible to conclude that for all four types of movement there are deviations between the measured and modeled electrical power or energy consumption. The deviations are highest for the rotation of the AGV and lowest for the translatory movement. Since typically the proportion of translatory motion in the overall movement sequence is significantly higher, the model developed in this project can be applied in factory planning or production planning, in particular to include the electrical energy requirements of AGVs in the energy efficiency evaluation.

6 Conclusion

In the context of energy system transformation, it is necessary to increase energy efficiency in all sectors in order to reduce primary energy demand. The industry sector has a great potential for this, and with the advancing developments in technologies, this potential can be exploited. However, it is essential to know the energy requirements of the individual operating resources. Since automated guided vehicles occupy an important part in new concepts of intralogistics, their energy requirements are investigated.

The objective is to develop a model that represents the electrical energy requirements of automated guided vehicles. For this purpose, an exemplary transport vehicle is first examined experimentally. The *RB1 Base* of the company *Robotnik* is utilized as application example. This is an underride vehicle. During the experiments the electrical power output of the battery is measured. This results in different movement modules for the three typical motion types of a vehicle. This includes the translational and rotational movement as well as the lifting and lowering movement of the load-carrying platform. The three movement modules for the translatory and rotatory movement are acceleration, driving at constant speed and braking. The lifting and lowering can be classified

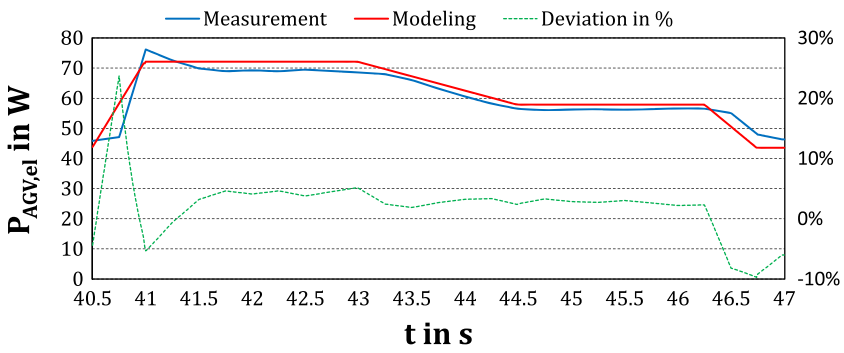

Fig. 27 Comparison between the measured values and the simulated values regarding the electrical power of the lowering movement ($v_{\text{Lift}} = 0.005\,\text{m/s}$, $m_{\text{Load}} = 37.795\,\text{kg}$, $s_{\text{Lift}} = 0.035\,m$)

in respectively five movement modules. For the lifting motion these are the modules acceleration, lifting without load, lifting load absorption, lifting under full load and braking. Regarding the lowering movement the modules are acceleration, lowering under full load, lowering load discharge, lowering without load and braking.

The experiments show that the electrical power requirement increases with the payload weight. Similarly, the power requirement rises with increasing speed for both translational and rotational motion. At the same time, however, the driving time decreases with rising speed. An analysis of the energy demand shows that the energy consumption of the automated guided vehicle reduces with increasing speed. Consequently, it is most energy efficient when a transport process is performed at maximum speed.

The results obtained from the experiments are used to simulate the electrical power and energy requirements of automated guided vehicles. First, the different identified movement modules are modeled by physical laws. These equations are then transferred into state flow graphs. These are implemented to be applied in the context of an event-discrete factory simulation, as this type of factory simulation is often used. This type of modeling is used to develop a general simulation model for underride vehicles. For other underride vehicle than the *RB1 Base* this model can be parameterized depending on their technical properties. However, this simulation model is not applicable to other types of automated guided vehicles. For example, load-carrying vehicles as autonomous forklift trucks have different movement modules than underride vehicles. Consequently, load-carrying vehicles can not be represented by this simulation model. This results in a continuing need for research in order to model other types of automated guided vehicles using appropriate simulation models.

The validation of the simulatively determined power profiles in relation to the recorded measurement values shows that the deviations are only slight. Consequently, the established simulation model can be used, for example, to integrate the electrical power and energy requirements of automated guided vehicles in production planning. This can improve the energy efficiency of intralogistics processes and thus the efficiency of entire production systems. By increasing efficiency and reducing lead times, products can be manufactured and delivered to customers faster and more efficiently. This results in an economic advantage for the company.

The main focus of the modeling is on the electrical power requirements of the motors of an automated guided vehicle. The other electrical consumers, such as the embedded-PC, the microcontroller and the sensors are not considered in detail. For these components, only the combined power demand is determined from an idling experiment and considered as a base load in the simulation model. For a more precise observation it would be of interest to measure the power requirements of the separate components independently of each other and to model them accordingly. The integrated-PC is of particular interest here. In actual investigations, the automated guided vehicle was controlled manually so that the PC did not have to perform high-level tasks such as route planning. In real factory operation, however, the execution of such tasks would increase the electrical power demand and therefore requires further analysis.

Furthermore, the acceleration power has not been taken into account in the modeling of the movement modules for the lifting and lowering operation, as not all the necessary data is available to calculate it. Consequently, further investigations are also of interest in order to represent the electrical power requirements more accurately.

Another important aspect regarding the power and energy requirements of automated guided vehicles is the consideration of the accumulator. This has not been examined in detail within the scope of the studies carried out so far. The state of charge is especially important for the operational planning of automated guided vehicles in production operations, as the charging time phases must be taken into account. With regard to the *RB1 Base*, which is used as an application example, it has a storage capacity of $Q_{\mathrm{Akku}} = 30\,\mathrm{Ah}$. According to the manufacturer, a continuous working time of 10 h is thus realizable. Since the control was performed manually during the experiments, no analysis and consequently no modeling of the discharge of the battery was done. This is however of interest for future investigations.

Within the framework of the experiments and modeling, the influencing factor temperature, as described in [22], has not been considered. In [22], it is shown that the energy requirement is reduced with increasing temperature, i.e. with warmed up automated guided vehicles. For this purpose, a detailed investigation of the influence of temperature on the power demand would be relevant in the future. Especially the influence on the movement modules acceleration and braking are of interests.

In summary, the developed model offers the possibility of realistically representing the electrical power and energy requirements of automated guided vehicles. By applying the model, the energy consumption of automated guided vehicles can be considered when evaluating the energy efficiency of production processes. A first application has been done in [48], where two logistics systems are compared with each other regarding their efficiency.

Acknowledgments Open Access funding provided by Projekt DEAL.

Funding information The project was funded by the Deutsche Forschungsgemeinschaft (DFG, German Research Foundation) - 276879186.

References

1. Federal Ministry for Economic Affairs and Energy (2014) Making more out of energy. National action plan on energy efficiency, Berlin, Germany
2. Federal Ministry for the Environment NatureConservation Building and Nuclear Saftey (2014) The german goverment's climate action programme 2020, Berlin, Germany
3. European Council (2014) Euco 169/14 Brussels, Belgium, European Council. https://www.consilium.europa.eu/uedocs/cms_data/docs/pressdata/de/ec/145424.pdf
4. Bunse K, Vodicka M, Schönsleben P, Brüllhart M, Ernst FO (2011) Integrating energy efficiency performance in production management, Gap analysis between industrial needs and scientific literature. J Clean Prod 2011(19):667–679
5. Leobner I, Ponweiser K, Neugschwandtner G, Kastner W (2011) Energy efficient production, A holistic modeling approach. In: 2011 World Congress on Sustainable Technologies, London, Great Britain, pp 62–67
6. Javied T, Bakakeu J, Gessinger D, Franke J (2018) Strategic energy management in industry 4.0 environment. In: 2018 Annual IEEE International Systems Conference (SysCon), Vancouver, Canada, pp 1–4
7. Delbrügger T, Döbbeler F, Greafenstein J, Lager H, Lenz L, Meßner M, Müller D, Regelmann P, Scholz D, Schumacher C, Winkels J, Wirtz A, Zeidler F (2017) Anpassungsintelligenz von fabriken im dynamischen und komplexen umfeld. ZWF - Zeitschrift für wirtschaftlichen Fabrikbetrieb 2017(6):364–368
8. Shrouf F, Ordieres J, Miragliotta G (2014) Smart factories in industry 4.0, A review of the concept and of energy management approached in production based on the internet of things paradigm. In: 2014 IEEE International Conference on Industrial Engineering and Engineering Management, Malaysia, pp 697–701
9. Ishida T, Yokoo M, Gasser L (2008) An organizational approach to adaptive production systems. In: AAAI-90 Proceedings, pp 52–58
10. Fraunhofer Institute for Production Technology (IPT) (2017) Industrie 4.0 Vernetzte, adaptive produktion. https://www.ipt.fraunhofer.de/de/trendthemen/industrie40.html
11. Sinorkyan D, Armbruster C (2016) Connected solution Energy efficiency for manufacturing enterprises. In: VDE-Kongress 2016, Mannheim, Germany, pp 1–5
12. Brauckmann O (2015) Smart production: Wertschöpfung durch geschäftsmodelle, 1st edn. Springer Vieweg, Berlin
13. Bauernhansel T, ten Hompel M, Vogel-Heuser B (2014) Industrie 4.0 in produktion, automatisierung und logistik: Anwendung, technologien und migration, 1st edn. Springer Vieweg, Berlin
14. (2008) Wandlungsfähige produktionssysteme Heute die industrie von morgen gestalten, Peter Nyhuis and Gunther Reinhart and Eberhard Abele
15. Kasilingam RG, Gobal SL (1996) Vehicle requirements model for automated guided vehicle systems. The International Journal of Advanced Manufacturing Technology 1996(12):276–279
16. Ilic OR (1994) Analysis of the number of automated guided vehicles required in flexible manufacturing systems. The International Journal of Advanced Manufacturing Technology 1994(9):382–389
17. Umar UA, Ariffin MKA, Ismail N, Tang SH (2015) Hybrid multiobjective genetic algorithms for integrated dynamic scheduling and routing of jobs and automated-guided vehicle (AGV) in flexible manufacturing systems (FMS) environment. The International Journal of Advanced Manufacturing Technology 2015(81):2123–2141
18. Yin X-H, Zhao H (2013) On a new sectionalized motion control strategy for automated guided vehicles: modeling and simulation validation. The International Journal of Advanced Manufacturing Technology 2013(69):637–646
19. Yan R, Jackson LM, Dunnett SJ (2017) Automated guided vehicle mission reliability modelling using a combined fault tree and petri net approach. The International Journal of Advanced Manufacturing Technology 2017(92):1825–1837
20. Qiu L, Wang J, Chen W, Wang H (2015) Heterogenus AGV routing problem considering energy consumption. In: 2015 IEEE International Conference on Robotics and Biomimetics (ROBIO), pp 1894–1899
21. Kim S, Jin H, Seo M, Har D (2019) Optimal path planning of automated guided vehicle using dijkstra algorithm under dynamic conditions. In: 2019 7th International Conference on Robot Intelligence Technology and Application (RiTA), pp 231–236
22. Riazi S, Bengtsson K, Lennartson B (2020) Energy optimization of large-scale agv systems. In: IEEE Transactions on automation science and engineering, pp 1–12, https://doi.org/10.1109/TASE.2019.2963285
23. Martin H (2016) Transport- und lagerlogistik Systematik, planung, einsatz und wirtschaftlichkeit, 10th edn. Springer Vieweg, Berlin
24. Muchna C, Brandenburg H, Fottner J, Gutermuth J (2018) Grundlagen der logisitk Begriffe, strukturen und prozesse, 1st edn. Springer Gabler, Wiesbaden, Germany
25. Pfohl H-C (2018) Logistiksysteme Betriebswirtschaftliche grundlagen, 9th edn. Springer Vieweg, Berlin, Heidelberg, Germany
26. Pfohl H-C (2016) Logistikmanagement Konzeption und funktionen, 3rd edn. Springer Vieweg, Berlin, Heidelberg, Germany
27. Günter U (2014): *Eine fibel mit praxisanwendung zur technik für die planung* Fahrerlose transportsysteme, 2nd edn. Springer Vieweg, Berlin
28. Maurer M, Gerdes JC, Lenz B, Winner H (2015) Autonomes fahren Technische, rechtliche und gesellschaftliche aspekte, 2nd edn. Springer Vieweg, Berlin
29. The Association of German Engineers (2009) Infrastructure and peripheral installations for automated guided vehicle systems (agvs). Beuth Verlag, Berlin
30. Mei Y, Lu Y-H, Hu YC, Lee CSG (2005) A case study of mobile robot's energy consumption and conservation techniques. In: Proceedings of the 12th International Conference on Advanced Robotics, Seattle, Washington, USA, pp 492–497
31. Larminie J, Lowry J (2012) Electric vehicle technology explained, 2nd edn. John Wiley & Sons Ltd, New Jersey
32. Fischer R (2017) Elektrische maschinen, 17th edn. Carl Hanser Verlag, München, Germany
33. Doeuff RL, Zaim MEH (2010) Rotating electrical machines, 1st edn. John Wiley & Sons, Inc, Hoboken, New Jersey, USA

34. Specovius J (2018) Grundkurs leistungselektronik Bauelemente, schaltungen und systeme, 9th edn. Springer Vieweg, Wiesbaden, Germany
35. Peddapelli SK (2017) Pulse width modulation Analysis and performance in multilevel inverters, 1st edn. De Gruyter, Oldenbourg, Germany
36. Robotnik (2015) Data sheet - rb1 base. https://www.robotnik.eu/web/wp-content/uploads//2015/11/Robotnik_DATASHEET_RB-1-BASE_EN.pdf
37. Robotnik (2018) Robotnik automation / rb1_base_common. https://github.com/RobotnikAutomation/rb1_base_common/blob/kineticdevel/rb1_base_control/config/rb1_base_control.yaml
38. Habenicht S, Ertl R, a. Günther W (2013) Analytische Energiebedarfsbestimmung von Intralogistiksystemen in der Planungsphase. Logisitics Journal 2013(10):1–14
39. Rudolph M, Wagner U (2008) Energieanwendungstechnik Wege und mäglichkeiten zur optimierung der energietechnik, 1st edn. Springer, Berlin
40. Mejri E, Kelouwani S, Dube Y, Trigui O, Agbossou K (2017) Energy efficiency path planning for low speed autonomous electric vehicle. In: Proceedings of the IEEE Vehicle Power and Propulsion Conference (VPPC), Belfort, France, pp 1–6
41. Garbrecht F, Schäfer J (1996) Das 1x1 der antriebsauslegung Wegweiser für anfänger und profis, 2nd edn. VDE-Verlag, Berlin, Germany
42. Weck M, Brecher C (2006) Werkzeugmaschinen 3 Mechatronische systeme, vorschubantriebe, prozessdiagnose, 6th edn. Springer Vieweg, Berlin, Heidelberg, Germany
43. Stross (2011) SERVOMECH Trapezspindel Getriebe. https://www.stross.de/files/catalogs/Spindelhubgetriebe.pdf
44. Feng L, Ulutan D, Mears L (2015) Energy consumption modeling and analyses in automotive manufacturing final assembly process. In: 2015 IEEE Conference on Technologies for Sustainability, Greenville, South Carolina, USA, pp 224–228
45. Larek R, Brinksmeier E, Meyer D, Pawletta T, Hagendorf O (2011) A discrete-event simulation approach to predict power consumption in machining processes. Production Engineering Research and Development 5(5):575–579
46. Beier J (2017) Simulation approach towards energy flexible manufacturing systems, 1st edn. Springer International Publishing, Cham, Switzerland
47. Delbrügger T, Meißner M, Wirtz A, Wiederkehr P, Rossmann J, Myrzik J, Biermann D (2019) Multi-level simulation concept for multi-disciplinary analysis and optimization of production systems. The International Journal of Advanced Manufacturing Technology 103(9):3993–4012
48. Meißner M (2020) Entwicklung eines energieeffizienzzyklus für adaptive produktionssysteme, Ph.D. Thesis. TU Dortmund University